Complex Fourier demodulation approach for the dual rotation polarizer-analyzer polarimeter

J. Cervantes-L.
University Center for Exact Sciences and Engineering, Guadalajara University, Blvd. Gral. Marcelino García Barragán 1421, Olímpica, Guadalajara, Jal, C.P. 44430.

G. A. Parra Escamilla
Universidad Panamericana. Facultad de Ingeniería, Álvaro del Portillo 49, Zapopan, Jalisco, 45010, México, University Center for Exact Sciences and Engineering, Guadalajara University, Blvd. Gral. Marcelino GarcÃa Barragán 1421, Olímpica, Guadalajara, Jal, C.P. 44430.

J. L. Flores Núñez
University Center for Exact Sciences and Engineering, Guadalajara University, Blvd. Gral. Marcelino García Barragán 1421, Olímpica, Guadalajara, Jal, C.P. 44430.

D. I. Serrano García
University Center for Exact Sciences and Engineering (CUCEI), Guadalajara University, Blvd. Gral. Marcelino García Barragán 1421, Olímpica, Guadalajara, Jal, C.P. 44430.

Received 31 August 2022; accepted 20 October 2022

In this research, we propose a demodulation algorithm for the dual rotation polarizer-analyzer polarimeter. The proposal retrieves the partial Mueller matrix from the complex coefficients, theoretically calculated from the Fourier transform of the output intensity. As calibration parameters, the initial orientations of the polarizer-analyzer are used. Experimental results for air and a rotating dichroic film polarizer show our proposal's feasibility.

Keywords: Polarized light; Mueller matrix; optical instrumentation.

DOI: https://doi.org/10.31349/RevMexFis.69.031301

1. Introduction

Polarimetry is an experimental technique focused on determining the optical properties of samples by analyzing the polarization response of the light reflected or transmitted by a sample. It has been helpful to develop new measurement systems; for example, in the last decade, the atmospheric sensing field has used polarization measurements to characterize the pollution particles in the environment [1,2] and sense climate variations [3]. In remote sensing detection, polarized light also analyzes reflective objects such as metals, and glasses, among other materials [4]. In the biomedical field, it has been proposed as a marker to identify cancerous tissue in its early stages [5]. In the ophthalmic field, researchers combine polarization with OCT techniques for retinal imaging implementations [6,7].

Several designs of polarimeters can be found in the literature, for example, by using a dual rotating retarder configuration [8,9], employing phase modulators [10], or liquid crystal retarders [11,12]. The dual rotating retarder configuration is a well-known polarimeter composed of a fixed polarizer, analyzer, and two rotating linear retarders [9,13-15]. The dual rotating retarder system measures the complete Mueller matrix by analyzing the frequency response obtained through the rotation of the retarders.

The Mueller matrix decomposition algorithms separate the information into three parameters associated with the sample's physical properties as diattenuation, retardance, and depolarization [16-18]. Diattenuation describes the polarization dependence of attenuating the light, which helps to describe scattering and chirality information. Retardance represents the phase variation dependence where its circularity is useful for glucose measurements, and its linearity is associated with stress analysis. Depolarization is the ability to maintain the polarization properties of the light, and its commonly used for cancer detection [5-7].

Another type of polarimeter employs a rotating polarizer and analyzer without linear retarders. Azzam R.M.A firstly proposed this polarimeter [19], where he showed theoretically the feasibility of the implementation and its capabilities to retrieve the partial Mueller matrix and Jones matrix coefficients through common transformations. Later, several authors followed Azzam's approach to retrieve the ellipticity parameter through the Jones Matrix approximation, mainly applied for thin film analysis [20-22] at several wavelength regions [23]. Similarly, other authors used the Jones matrix approach to retrieve ellipticity phase information [24,25], which was improved later by adding a compensator to the system [26]. Although several authors proposed the rotating polarizer-analyzer system, the analysis from the complex

Fourier coefficients, as far as we know, which is the main objective of our research, has not been carried out.

The main goal of our proposal is to consider the complex Fourier transform coefficients of the intensity signal to retrieve the partial Mueller matrix and take the initial angles as calibration parameters. The paper first explains the demodulation algorithm continuing with experimental results of our implementation and ending with our conclusions. The approach presented in this paper can improve other polarimetric systems by considering the theoretical response of the Fourier transform of the output intensity.

2. Complex Fourier demodulation algorithm

The approach for retrieving the partial Mueller matrix using a dual rotating polarizer-analyzer is composed firstly of a polarization state generator with a light source working at wavelength λ, a linear polarizer LP(0°) oriented at angle 0° (used as an orientation reference) and a linear polarizer LP($\theta+\varepsilon_1$), rotating at rate 4θ with an initial angle at ε_1. The polarization state detection unit consists of a linear polarizer LP($4\theta+\varepsilon_2$) rotating at a rate 4θ with an initial angle of ε_2 and an intensity detector that could be a camera or a photodetector. The sample is mathematically represented as a Mueller matrix with 16 coefficients, but as we are employing two rotating polarizers, only a partial Mueller matrix can be retrieved. Figure 1 shows the diagram and the theoretical parameters involved in the system.

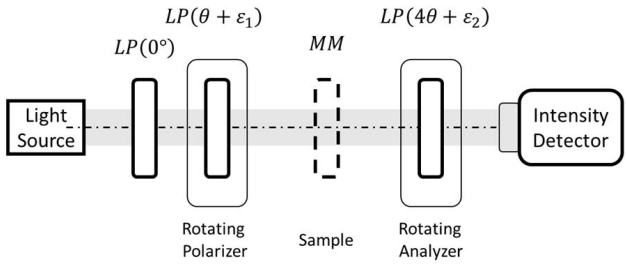

FIGURE 1. Rotating polarizer-analyzer polarimeter composed of a light source; a polarizer LP(0°) oriented at 0° used as an orientation reference; a rotating polarizer LP($\theta+\varepsilon_1$) at rate θ and initial angle ε_1; a rotating analyzer LP($4\theta+\varepsilon_2$) at rate 4θ and initial angle ε_2; and an intensity detector that could be a camera or a photodetector.

The Mueller matrix of a linear polarizer LP(θ) for a given angle θ is represented as [17,18].

$$LP(\theta)=\frac{1}{2}\begin{pmatrix}1 & \cos(2\theta) & \sin(2\theta) & 0\\ \cos(2\theta) & \cos^2(2\theta) & \cos(2\theta)\sin(2\theta) & 0\\ \sin(2\theta) & \cos(2\theta)\sin(2\theta) & \sin^2(2\theta) & 0\\ 0 & 0 & 0 & 0\end{pmatrix}, \tag{1}$$

while a general Mueller matrix (MM) is given by

$$MM=\begin{pmatrix}m_{11} & m_{12} & m_{13} & m_{14}\\ m_{21} & m_{22} & m_{23} & m_{24}\\ m_{31} & m_{32} & m_{33} & m_{34}\\ m_{41} & m_{42} & m_{43} & m_{44}\end{pmatrix}, \tag{2}$$

Considering non-polarized light as input, $S_{\text{in}}=[S_0,0,0,0]^T$ where S_0 represents the total incoming intensity. The output Stokes vector, S_{out}, is

$$S_{\text{out}}=LP(4\theta+\varepsilon_2)\cdot MM\cdot LP(\theta+\varepsilon_1)\cdot LP(0)\cdot S_{\text{in}}. \tag{3}$$

The total detected intensity, I_{out} is the first element of S_{out} calculated as

$$\begin{aligned}I_{\text{out}}(\theta)=\frac{S_0}{16}\Big[&(2m_{11}+m_{12})+2(m_{11}+m_{12})\cos(2\varepsilon_1+2\theta)+2m_{13}\sin(2\varepsilon_1+2\theta)+m_{12}\cos(4\varepsilon_1+4\theta)\\ &+m_{13}\sin(4\varepsilon_1+4\theta)+(2m_{21}+m_{22})\cos(2\varepsilon_2+8\theta)+(2m_{31}+m_{32})\sin(2\varepsilon_2+8\theta)+(m_{21}+m_{22}-m_{33})\\ &\times\cos(2(\varepsilon_1+\varepsilon_2)+10\theta)+(m_{23}+m_{31}+m_{32})\sin(2(\varepsilon_1+\varepsilon_2)+10\theta)+\frac{1}{2}(m_{22}-m_{33})\cos((2(2\varepsilon_1+\varepsilon_2)\\ &+12\theta)+\frac{1}{2}(m_{32}+m_{23})\sin(2(2\varepsilon_1+\varepsilon_2)+12\theta)+\frac{1}{2}(m_{22}+m_{33})\cos(2(2\varepsilon_1-\varepsilon_2)-4\theta)+\frac{1}{2}(m_{23}\\ &-m_{32})\sin((2(2\varepsilon_1-\varepsilon_2)-4\theta)+(m_{21}+m_{22}+m_{33})\cos((2\varepsilon_1-\varepsilon_2)-6\theta)\\ &+(m_{23}-m_{31}-m_{32})\sin((2\varepsilon_1-2\varepsilon_2)-6\theta)\Big].\end{aligned} \tag{4}$$

TABLE I. Complex coefficients obtained from the Fourier transform of the output signal of the polarimeter.

$C_0 = (2m_{11} + m_{12})$	
$C_{-2} = e^{-2i\varepsilon_1}(m_{11} + m_{12} + im_{13})$	$C_{+2} = e^{2i\varepsilon_1}(m_{11} + m_{12} - im_{13})$
$C_{-4} = \frac{1}{4}e^{-2i(2\varepsilon_1+\varepsilon_2)}(2e^{2i\varepsilon_2}(m_{12} + im_{13}))$ $+e^{8i\varepsilon_1}(m_{22} - im_{23} + im_{32} + m_{33})$	$C_{+4} = \frac{1}{4}e^{2i(2\epsilon_1+\epsilon_2)}(2e^{-2i\epsilon_2}(m_{12} - im_{13})$ $+e^{-8i\epsilon_1}(m_{22} + im_{23} - im_{32} + m_{33}))$
$C_{-6} = \frac{1}{2}e^{2i(\varepsilon_1-\varepsilon_2)}(m_{21} + m_{22}$ $-im_{23} + im_{31} + im_{32} + m_{33})$	$C_{+6} = \frac{1}{2}e^{-2i(\varepsilon_1-\varepsilon_2)}(m_{21} + m_{22}$ $+im_{23} - im_{31} - im_{32} + m_{33})$
$C_{-8} = \frac{1}{2}e^{-2i\varepsilon_2}(2m_{21} + m_{22} + i(2m_{31} + m_{32}))$	$C_{+8} = \frac{1}{2}e^{2i\varepsilon_2}(2m_{21} + m_{22} - i(2m_{31} + m_{32}))$
$C_{-10} = \frac{1}{2}e^{-2i(\varepsilon_1+\varepsilon_2)}(m_{21} + m_{22} - m_{33}$ $+i(m_{23} + m_{31} + m_{32}))$	$C_{+10} = \frac{1}{2}e^{2i(\varepsilon_1+\varepsilon_2)}(m_{21} + m_{22} - m_{33}$ $-i(m_{23} + m_{31} + m_{32}))$
$C_{-12} = \frac{1}{4}e^{-2i(2\varepsilon_1+\varepsilon_2)}(m_{22} - m_{33} + i(m_{23} + m_{32}))$	$C_{+12} = \frac{1}{4}e^{2i(2\varepsilon_1+\varepsilon_2)}(m_{22} - m_{33} - i(m_{23} + m_{32}))$

We can take each element of the Mueller matrix of the sample as m_{ij}, θ is related to the rotation rate of the polarizer and $(\varepsilon_1, \varepsilon_2)$ are their initial angle used for calibration purposes. The detected signal modulated by the rotation rates of the polarizer-analyzer consist of a series of harmonics. The typical approach for retrieving the sample information is employing the Fourier series to calculate each coefficient of the sine-cosine terms in Eq. 4. In our proposal, we apply the Fourier transformation to the output signal to operate directly with the complex coefficients. The Fourier transform of the output intensity is composed of frequency-shifted Dirac delta functions where its complex coefficients are used for the demodulation. By considering the Fourier transform of a cosine function as

$$F\{\cos(\beta \pm n\theta)\}(\omega) = \frac{1}{2}[e^{\mp i\beta}\delta(\omega - n) + e^{\pm i\beta}\delta(\omega + n)],$$
$$F\{\sin(\beta \pm n\theta)\}(\omega) = \frac{1}{2}[e^{\mp i\beta}\delta(\omega - n) - e^{\pm i\beta}\delta(\omega + n)], \quad (5)$$

where β is the initial angle, n is the harmonic coefficient, $\delta(\omega \pm n)$ is the shifted Dirac delta function and ω the frequency domain. The Fourier transform of the intensity detected $\hat{I}_{\text{out}}(\omega)$ at Eq. 4 can be obtained as

$$\hat{I}_{\text{out}}(\omega) = \frac{S_0}{16}\sum_{k=-6}^{6} C_{2k}\delta(\omega + 2k), \quad (6)$$

where C_{2k} represents the complex coefficient dependent on the sample information and the initial angle of the polarizer ε_1 and analyzer ε_2. The function $\delta(\omega + 2k)$ represents the Dirac delta function displaced at each $2k$ frequency order. Table I shows each complex coefficient, and it is worth mentioning that the initial angle of the polarizer-analyzer represents a constant phase variation.

One of the advantages of our proposal is that it is possible to isolate the initial angles of the polarizer and analyzer $(\varepsilon_1, \varepsilon_2)$ as they behave as a common phase value in each complex Fourier coefficient. In this manner, the complex coefficients without initial angle information are

$$\alpha_{\pm 2} = \frac{1}{2}(e^{-2i\varepsilon_1}C_{+2} \pm e^{2i\varepsilon_1}C_{-2}),$$
$$\alpha_{\pm 6} = \frac{1}{2}(e^{-2i(\varepsilon_2-\varepsilon_1)}C_{+6} \pm e^{2i(\varepsilon_2-\varepsilon_1)}C_{-6}),$$
$$\alpha_{\pm 8} = \frac{1}{2}(e^{-2i\varepsilon_2}C_{+8} \pm e^{2i\varepsilon_2}C_{-8}),$$
$$\alpha_{\pm 10} = \frac{1}{2}(e^{-2i(\varepsilon_1+\varepsilon_2)}C_{+10} \pm e^{2i(\varepsilon_1+\varepsilon_2)}C_{-10}),$$
$$\alpha_{\pm 12} = \frac{1}{2}(e^{-2i(2\varepsilon_1+\varepsilon_2)}C_{+12} \pm e^{2i(2\varepsilon_1+\varepsilon_2)}C_{-12}). \quad (7)$$

As we are employing two rotating polarizers, we could retrieve a partial Mueller matrix where its coefficients are

TABLE II. Mueller matrix obtained with no-sample conditions non-compensated (M_{nc}), and the Mueller matrix compensated (M_c); additionally, the square error compared with the ideal Mueller matrix.

Non-Compensated	Compensated	Sum of Square Error(E)
$M_{nc} = \begin{pmatrix} 1.000 & -0.835 & 0.550 & X \\ 0.016 & 0.282 & 0.456 & X \\ -0.017 & -0.437 & -0.370 & X \\ X & X & X & X \end{pmatrix}$	$M_{nc} = \begin{pmatrix} 1.000 & -0.025 & 0.000 & X \\ -0.032 & 1.029 & 0.003 & X \\ -0.014 & 0.028 & 0.986 & X \\ X & X & X & X \end{pmatrix}$	0.003

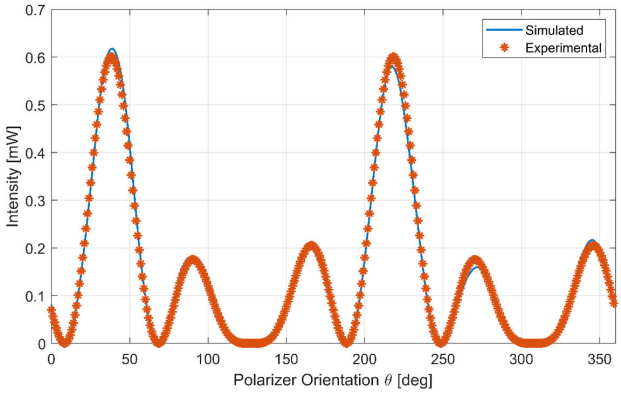

FIGURE 2. Intensity detected with a misalignment of $\varepsilon_1 = -36.676^\circ$ for the polarizer and $\varepsilon_2 = 28.117^\circ$ for the analyzer.

$$
\begin{aligned}
&m_{11} = C_0 - \alpha_{+2}, \qquad m_{12} = -C_0 + 2\alpha_{+2},\\
&m_{13} = i\alpha_{-2}, \qquad m_{21} = 2\alpha_{+10} - 4\alpha_{+12},\\
&m_{22} = 2\alpha_{+8} + 8\alpha_{+12} - 4\alpha_{+10} \qquad m_{23} = i(\alpha_{-10} - \alpha_{-6}),\\
&m_{31} = i(2\alpha_{-10} - 4\alpha_{-12}),\\
&m_{32} = i(2\alpha_{-8} - 4\alpha_{-10} + 8\alpha_{-12}),\\
&m_{33} = \alpha_{+6} - \alpha_{+10}.
\end{aligned} \tag{8}
$$

The initial angles of the polarizer-analyzer $(\varepsilon_1, \varepsilon_2)$ need to be measured beforehand by running a measurement without a sample and considering air as a non-polarizing sample. Therefore, the calibration parameters are

$$
\begin{aligned}
\tan(2\varepsilon_1) &= \frac{-i(C_{\text{air}+2} - C_{\text{air}-2})}{C_{\text{air}+2} + C_{\text{air}-2)}},\\
\tan(2\varepsilon_2) &= \frac{-i(C_{\text{air}+8} - C_{\text{air}-8})}{C_{\text{air}+8} + C_{\text{air}-8)}}.
\end{aligned} \tag{9}
$$

As a result, we can retrieve the partial Mueller matrix considering the complex Fourier coefficients directly where the initial angles of the polarizer and analyzer need to be measured beforehand, and they are a constant phase variation on the Fourier space.

3. Experimental results

To check the feasibility of our proposal, we built an experimental setup based on the dual rotating polarizer-analyzer polarimeter as presented in Fig. 1. The system utilizes a He-Ne laser light source working at 632.8 nm (Thorlabs-HNLS008L); as a first polarizer and orientation reference, we used a Wollaston prism to produce s-polarized light (Thorlabs-WP10) with a 20° beam separation and extinction ratio of 1:100,000 according to the manufacturer. For the polarizer and analyzer components, we employed two dichroic film polarizers mounted on a motorized rotation device (Thorlabs - K10CR1) and as an intensity detector, a USB power meter (Thorlabs - PM16-121) composed of a silicon photodiode sensor. The system was aligned and built according to the 30 mm Thorlabs optical cage system.

We obtained the partial Mueller matrix with no-sample conditions for the first set of experiments, where the polar-

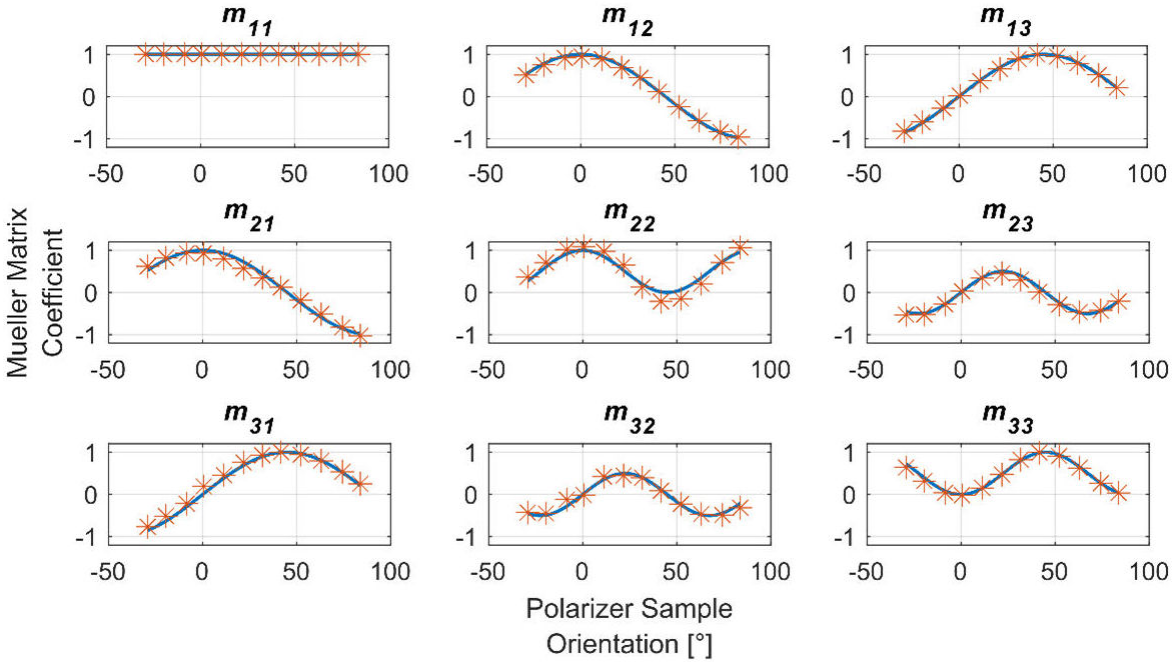

FIGURE 3. Variation of the partial Mueller matrix of a rotating dichroic film polarizer as a sample; asterisks represent the experimental results while the continuous line the simulated.

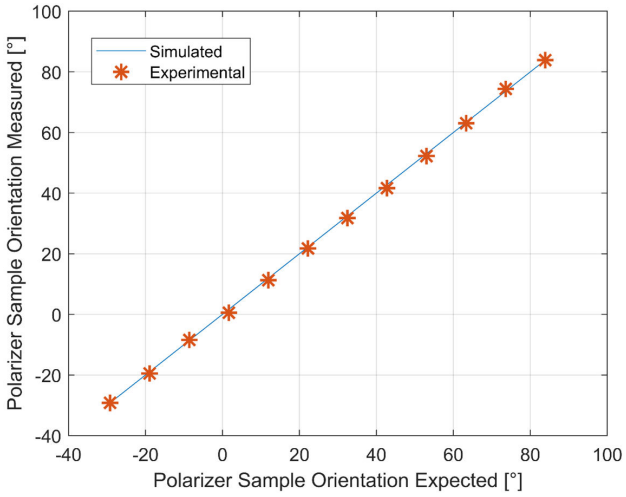

FIGURE 4. Comparison of the angle variation measured as a function of the expected value of the polarizer.

TABLE III. Root Mean Square Errors between the experimental and simulated value of the rotating dichroic film polarizer.

Root Mean Square Errors
$M_{RMSE} = \begin{pmatrix} 0 & 0.028 & 0.019 & X \\ 0.080 & 0.128 & 0.052 & X \\ 0.077 & 0.064 & 0.038 & X \\ X & X & X & X \end{pmatrix}$

izer and analyzer present a minor misalignment. We acquired 360 intensities by rotating the polarizers with an increment of one degree for the first polarizer and four degrees for the second polarizer sequentially. Figure 2 shows the intensity detected where the initial angles obtained by Eq. (9) are $\varepsilon_1 = -36.676°$ for the polarizer and $\varepsilon_2 = 28.117°$ for the analyzer, asterisks represent the experimental results while the continuous line is the simulated signal. Table II shows the partial Mueller matrices for the non-compensated and compensated cases, where the square error is

$$E = \sum_{i=1}^{3}\sum_{j=1}^{3}(m_{\exp_{ij}} - m_{meas_{ij}})^2 = 0.003$$

by comparing each coefficient (i, j) of the expected, $m_{\exp}$ and measured, m_{meas} Mueller matrix obtained after initial angle calibration.

In the second experiment, we considered a sample that varies all the Mueller matrix coefficients; in this manner, our sample was a dichroic film polarizer rotated within a range of 120° with steps of 10°. Furthermore, we placed the film in a mechanical rotation mount (Thorlabs - CRM1T). Figure 3 shows the partial Mueller matrix coefficients, asterisks corresponding to the experimental value, and the theoretical approach's continuous line. Table III shows the Root Mean Square Error (RMSE), where the m_{13} coefficient presents the minimum deviation while the coefficient m_{22} represents the maximum deviation of the measurement.

By considering the Lu-Chipman decomposition [16], we can analyze the angular position of the polarizer through $\tan(2\theta) = m_{13}/m_{12}$. In this case, it corresponds to the angular position of the linear diattenuation parameter. Figure 4 shows the angular variation comparing the expected against the measured value resulting in a $RMSE = 0.651°$.

4. Conclusions and final remarks

We developed a demodulation algorithm for the rotating polarizer-analyzer configuration based on theoretically calculating the complex Fourier transform coefficients. We focused on retrieving the partial Mueller matrix and the initial angles of the polarizer and analyzer for calibration purposes. Considering the complex Fourier coefficients, the initial angles of the polarizer-analyzer represent a constant phase on each complex term that can be isolated and removed from the Mueller matrix coefficients. The theoretical approach presented has the potential to be implemented on other types of polarimeters. For example, by taking advantage of the complex Fourier transform coefficients on the dual rotating retarder polarimeter.

Disclosures

The authors declare no conflicts of interest.

1. G. Van Harten *et al.*, Atmospheric aerosol characterization with a ground-based SPEX spectropolarimetric instrument, *Atmospheric Measurement Techniques* **7** (2014) 4341.
2. D. Li *et al.*, Differentiation of soot particulates in air using polarized light scattering method, *Applied optics* **56** (2017) 4123.
3. J.-C. Roger *et al.*, Polarization of the solar light scattered by the earth-atmosphere system as observed from the US shuttle, *Remote sensing of environment* **48** (1994) 275.
4. G. Calvert, Application of modern automated photoelasticity to industrial problems, *Insight* **44** (2002) 224.
5. C. He *et al.*, Polarisation optics for biomedical and clinical applications: *a review, Light: Science & Applications* **10** (2021) 1.
6. H. Afsharan *et al.*, Polarization properties of retinal blood vessel walls measured with polarization sensitive optical coherence tomography, *Biomedical Optics Express* **12** (2021) 4340.
7. I. Meglinski, T. Novikova, and K. Dholakia, Polarization and Orbital Angular Momentum of Light in Biomedical Applications: feature issue introduction, *Biomedical Optics Express* **12** (2021) 6255.

8. R. Azzam, Photopolarimetric measurement of the Mueller matrix by Fourier analysis of a single detected signal, *Optics Letters* **2** (1978) 148.

9. D. H. Goldstein, Mueller matrix dual-rotating retarder polarimeter, *Applied optics* **31** (1992) 6676.

10. E. Compain and B. Drevillon, Complete high-frequency measurement of Mueller matrices based on a new coupled-phase modulator, *Review of scientific instruments* **68** (1997) 2671.

11. E. García-Caurel, A. De Martino, and B. Drevillon, Spectroscopic Mueller polarimeter based on liquid crystal devices, *Thin Solid Films* **455** (2004) 120.

12. B. Laude-Boulesteix *et al*., Mueller polarimetric imaging system with liquid crystals, *Applied optics* **43** (2004) 2824.

13. D. H. Goldstein and R. A. Chipman, Error analysis of a Mueller matrix polarimeter, *JOSA A* **7** (1990) 693.

14. K. Bhattacharyya, D. I. Serrano-García, and Y. Otani, Accuracy enhancement of dual rotating mueller matrix imaging polarimeter by diattenuation and retardance error calibration approach, *Optics Communications* **392** (2017) 48.

15. K. Twietmeyer and R. Chipman, Optimization of Mueller matrix polarimeters in the presence of error sources, *Optics Express* **16** (2008) 11589.

16. S.-Y. Lu and R. A. Chipman, Interpretation of Mueller matrices based on polar decomposition, *JOSA A* **13** (1996) 1106

17. D. H. Goldstein, *Polarized light* (CRC press, pp. 47, 2017).

18. R. Chipman, Polarimetry, Chapter 22, Handbook of Optics, Volume-II (1995).

19. R. Azzam, A simple Fourier photopolarimeter with rotating polarizer and analyzer for measuring Jones and Mueller matrices, *Optics Communications* **25** (1978) 137.

20. M. Gilliot and A. E. Naciri, Theory of dual-rotating polarizer and analyzer ellipsometer, *Thin solid films* **540** (2013) 46.

21. T. M. El-Agez and S. A. Taya, Development and construction of rotating polarizer analyzer ellipsometer, *Optics and lasers in engineering* **49** (2011) 507.

22. S. A. Taya and T. M. El-Agez, Effect of noise on the optical parameters extracted from different ellipsometric configurations, *Physica Scripta* **85** (2012) 045706

23. G.-Q. Xia, et al., New design of the variable angle infrared spectroscopic ellipsometer using double Fourier transforms, *Review of Scientific Instruments* **71** (2000) 2677.

24. S. Y. Berezhna, I. V. Berezhnyy, and M. Takashi, Dynamic photometric imaging polarizer-sample-analyzer polarimeter: instrument for mapping birefringence and optical rotation, *JOSA A* **18** (2001) 666.

25. S. Berezhna, I. Berezhnyy, and M. Takashi, Integrated photoelasticity through imaging Fourier polarimetry of an elliptic retarder, *Applied optics* **40** (2001) 644.

26. S. Berezhna, I. Berezhnyy, and M. Takashi, High-resolution birefringence imaging in three-dimensional stressed models by Fourier polarimetry, *Applied optics* **40** (2001) 4940.